

Article:

Valle, Beatriz; García-Gómez, Naiara; Remiro, Aingeru; Gayubo, Ana Guadalupe; Bilbao, Javier. **Cost-effective upgrading of biomass pyrolysis oil using activated dolomite as a basic catalyst.** *Fuel Processing Technology* 195: 106142 (2019)

Received 21 May 2019; Received in revised form 26 June 2019; Accepted 5 July 2019. Available online 19 July 2019

This work is made available online in accordance with publisher policies. To see the final version of this work please visit the publisher's website. Access to the published online version may require a subscription. Link to publisher's version:

<https://doi.org/10.1016/j.fuproc.2019.106142>

Copyright statement:

© 2019 Elsevier B.V. Full-text reproduced in accordance with the publisher's self-archiving policy. This manuscript version is made available under the CC-BY-NC-ND 4.0 license

<http://creativecommons.org/licenses/by-nc-nd/4.0/>



# Cost-effective upgrading of biomass pyrolysis oil using activated dolomite as a basic catalyst

Beatriz Valle\*, Naiara García-Gómez, Aingeru Remiro, Ana G. Gayubo and Javier Bilbao

*Department of Chemical Engineering, University of the Basque Country (UPV/EHU), P.O. Box 644, Bilbao 48080, Spain, Tel: +34946015361, Fax: +34946013500*

\* Corresponding author, e-mail: [beatriz.valle@ehu.eus](mailto:beatriz.valle@ehu.eus)

---

## ABSTRACT

This study deals with a continuous process on a calcined dolomite operating at atmospheric pressure and by co-feeding water for cost-effective upgrading of raw bio-oil at 400 °C and 500 °C. The distribution of carbon in the feed to the product fractions (gas and upgraded bio-oil) and to the dolomite (as CO<sub>2</sub> captured and coke) was investigated with time on stream, as well as the evolution of the gas and the upgraded bio-oil composition. Acids and high-molecular weight phenols were completely removed from the raw bio-oil for 0.5 h time on stream, with the upgraded bio-oil being mainly composed of ketones (acetone, 2-butanone and cyclopentanones). Chromatographic analyses of the reaction products were combined with analysis of the dolomite characteristics by thermogravimetry and X-ray diffraction. The results are explained on the basis of possible reaction mechanisms on the dolomite basic sites (CaO, Ca(OH)<sub>2</sub> and MgO) and the extent of dolomite carbonation with adsorbed CO<sub>2</sub>. The composition of the upgraded bio-oil is suitable for subsequent catalytic valorization for obtaining fuels and chemicals, and in particular for the production of hydrogen by steam reforming.

**KEYWORDS:** raw bio-oil, upgrading, basic catalyst, dolomite, ketonization

## 1 1. INTRODUCTION

2 Pyrolysis oil (bio-oil) is a complex mixture of oxygenated compounds and water that  
3 can be produced by fast pyrolysis of lignocellulosic biomass. This liquid product is very  
4 attractive for the sustainable production of automotive fuels, H<sub>2</sub> and chemicals through  
5 several thermo-chemical and catalytic processes [1, 2]. Furthermore, high yield of bio-oil  
6 can be obtained from biomass by means of simple, energy-efficient, and environmentally  
7 friendly pyrolysis technologies, which have reached a high level of development [3].  
8 However, storage, handle and conversion of raw bio-oil are hindered by its complex  
9 composition and poor properties (high oxygen content, thermal instability, acidity,  
10 corrosivity and low viscosity). Particularly, certain compounds (mainly phenols and  
11 acids) cause operational problems and catalyst deactivation in raw bio-oil valorization  
12 processes (e.g. cracking, hydrotreating and steam reforming) due to re-polymerisation  
13 and other undesirable reactions [4-7].

14 Consequently, many strategies have been addressed for converting the raw bio-oil into  
15 a high-quality and stable oil, whose further catalytic processing would be more feasible  
16 [8, 9]. These methods include: esterification, aldol condensation, ketonization, *in situ*  
17 catalytic cracking, and mild hydrodeoxygenation [2]. In this regard, a great variety of  
18 catalysts and reaction systems have been assessed on the basis of yield/purity of target  
19 products, reaction conditions severity, catalyst deactivation, feed-to-catalyst ratio, and  
20 catalyst cost [2, 9, 10]. The results point to the need for directing future research toward  
21 capital cost reduction by developing new catalysts and processes, eliminating operation  
22 units, decreasing reactor temperature and/or pressure, and finding sustainable sources for  
23 H<sub>2</sub> supply, etc. [10, 11]. Accordingly, the raw bio-oil conditioning by means of low-cost  
24 alternatives which employ cheap catalysts, waste products and/or naturally available  
25 elements [12, 13] is attracting increasing attention.

26 The catalytic pyrolysis of biomass using *in situ* CaO-based materials in the 450-500  
27 °C range has been reported to improve the bio-oil quality by reducing its acidity and  
28 increasing the heating value [14, 15]. Stefanidis et al. [16] have evaluated the use of MgO  
29 as a sustainable and low-cost alternative to HZSM-5 zeolite, and stated that acid content  
30 in the bio-oil was reduced via ketonization and aldol condensation reactions on the MgO  
31 basic sites.

32 Dolomitic rock is a naturally abundant and low-toxic calcium and magnesium  
33 carbonate (CaMg(CO<sub>3</sub>)<sub>2</sub>) that may contain impurities of Fe<sub>2</sub>O<sub>3</sub>. It has been extensively  
34 used as a catalyst in biomass gasification processes for reducing the tar formation by  
35 cracking and reforming the high-molecular-weight compounds. Thus, yield and quality  
36 of the syngas produced are improved [17-21]. Furthermore, the CaO and MgO basic sites  
37 of calcined dolomite are effective for deoxygenating the bio-oil produced by biomass  
38 pyrolysis, enhancing the cracking of heavy organics into lighter fractions so that more  
39 desirable compounds are formed [14, 22-24]. Specifically, carboxylic acids are converted  
40 into ketones *via* ketonization reactions, whereas the lignin derived oligomers are  
41 converted into less-oxygenated phenols and aromatics. Consequently, the resulting bio-

1 oil has lower acidity, higher calorific value and improved stability, and therefore, a greater  
2 potential for utilization and/or downstream upgrading.

3 The feasibility of raw bio-oil valorization requires production of value-added bio-oils  
4 with high content of target products. Given the high concentration of carboxylic acids  
5 (mainly acetic acid) in raw bio-oil, ketonization emerges as an attractive alternative for  
6 decreasing the oxygen content, while maximizing the content of ketones in bio-oil.  
7 Vapor-phase ketonization of carboxylic acids over a wide variety of metal oxides (e.g.,  
8  $\text{TiO}_2$ ,  $\text{ZrO}_2$ ,  $\text{SiO}_2$ ,  $\text{Al}_2\text{O}_3$ ,  $\text{MnO}_2$ ,  $\text{CeO}_2$ ,  $\text{CeZrO}_x$ ) has attracted extensive attention [9, 25,  
9 26]. However, most of the studies have focused on the conversion of pure oxygenates  
10 (bio-oil model compounds), and there are few studies that approach ketonization of  
11 oxygenates mixture (simulated bio-oil) and raw bio-oil [27-30]. Therefore, information  
12 regarding the interactions of acids with other raw bio-oil compounds is scarce.

13 The capability of calcined dolomite for removing carboxylic acids (mainly acetic and  
14 formic) from bio-oil at low temperature ( $\leq 500\text{ }^\circ\text{C}$ ) has been reported in a previous study  
15 on the steam reforming (SR) of a bio-oil/ethanol mixture [31]. These acids and other  
16 reactive compounds (e.g., levoglucosan, aldehydes, phenols), which cause catalyst  
17 deactivation and constraint the viability of the SR process, are converted into less-  
18 oxygenated compounds (mainly ketones and alkyl-phenols) through ketonization,  
19 esterification, demethylation, and dehydration reactions. The prevailing reactions are  
20 strongly influenced by the operating conditions (temperature and time on stream) with  
21 ketonization being enhanced below  $600\text{ }^\circ\text{C}$ .

22 The purpose of this paper is to assess the feasibility of a continuous catalytic upgrading  
23 of raw bio-oil using dolomite in a low-cost reaction system (atmospheric pressure,  
24 temperatures  $\leq 500\text{ }^\circ\text{C}$ , and without external  $\text{H}_2$  supply). Additional water was co-fed with  
25 the raw bio-oil for enhancing ketonization activity of the dolomite by promoting the  
26 formation of a  $\text{Ca}(\text{OH})_2$  strong basic phase. Suitable operating conditions of this original  
27 alternative are established for conditioning the raw bio-oil composition by removing  
28 undesirable compounds (carboxylic acids and phenols). The composition of the upgraded  
29 bio-oil (with high concentration of ketones) enables its subsequent further valorization  
30 (e.g., by steam reforming).

## 31 **2. EXPERIMENTAL**

### 32 **2.1. Bio-oil**

33 The raw bio-oil, provided by *BTG Bioliquids BV* (the Netherlands), was produced by  
34 flash pyrolysis of pine sawdust in an industrial plant with 5 t/h capacity and a conical  
35 rotary reactor. The elemental composition was analyzed using a *Leco CHN-932* analyzer  
36 and ultra-microbalance *Sartorius M2P*, and the water content was determined by Karl  
37 Fischer titration (*KF-Titrino Plus 870*). The contents of carbon (C), hydrogen (H), oxygen  
38 (O) and water in the raw bio-oil were 55.4 %, 6.2 %, 38.4 % and 26 wt%, respectively.

39 The chemical composition was analyzed using a *Shimadzu QP2010S* gas  
40 chromatography/mass spectrometer (GC/MS) provided with a BPX-5 column (50 m x

1 0.22 mm x 0.25  $\mu\text{m}$ ) and mass selective detector. The bio-oil compounds were grouped  
2 into families: acids, ketones, esters, furanes and furanones, alcohols, aldehydes, ethers,  
3 anhydrosugars, and phenols. Identification of compounds was accomplished by matching  
4 the mass spectra with those from *NIST 147* and *NIST 27* data libraries. Direct  
5 quantification of the bio-oil components by the usual calibrated peak area procedure could  
6 not be feasibly carried out from GCMS data due to the complexity of these compounds.  
7 Therefore, semi-quantitative method based on the chromatographic area percentage was  
8 used to determine the relative proportion of each compound. It should be pointed out that  
9 GC/MS technique has limited capability for detecting heavy oligomeric compounds with  
10 molecular weight greater than 320 g/mol [32].

## 11 **2.2. Characterization of natural, calcined and deactivated dolomite**

12 The dolomite used in this work was produced and supplied by *Calcinor S.A.*  
13 (Cantabria, Spain). It is a natural solid resource usually intended for agriculture,  
14 construction industry, and manufacturing refractory bricks. After being dried at 110  $^{\circ}\text{C}$   
15 for 12 h, the as-received natural dolomite was calcined at 850  $^{\circ}\text{C}$  for 5 h to transform it  
16 into active CaO/MgO phases. Thermal decomposition behavior of natural dolomite was  
17 analyzed using *TA Instruments Q5000 IR* thermobalance by heating the sample at 5  
18  $^{\circ}\text{C}/\text{min}$  up to 800  $^{\circ}\text{C}$  under a  $\text{N}_2$  atmosphere (10 ml/min). The temperature was held at  
19 800  $^{\circ}\text{C}$  for 10 min and then it was raised up to 900  $^{\circ}\text{C}$  and held for 10 min more.

20 The *TA Instruments Q5000 IR* thermobalance was also coupled to a mass spectrometer  
21 *Thermostar Balzers Instrument* for monitoring the signal corresponding to  $\text{CO}_2$ , with the  
22 aim of quantifying the amount of  $\text{CO}_2$  adsorbed and coke deposited on the deactivated  
23 dolomite after each experiment. For this purpose, a “calcination-combustion” method was  
24 developed: i) heating from 50  $^{\circ}\text{C}$  to 750  $^{\circ}\text{C}$  at 5  $^{\circ}\text{C}/\text{min}$  under inert atmosphere (10 ml/min  
25  $\text{N}_2$ ) in order to decompose  $\text{CaCO}_3$  into CaO thus releasing the adsorbed  $\text{CO}_2$  (calcination  
26 stage); ii) cooling the sample again to 50  $^{\circ}\text{C}$ ; and iii) heating from 50  $^{\circ}\text{C}$  up to 800  $^{\circ}\text{C}$  at  
27 5  $^{\circ}\text{C}/\text{min}$  under oxidizing atmosphere (60 ml/min air) in order to burn the coke deposited  
28 (combustion stage).

29 Crystalline phases of natural, calcined and deactivated dolomite samples were  
30 analyzed by a *D8 Advance* X-ray diffractometer (XRD). The XRD patterns were obtained  
31 over  $10^{\circ} \leq 2\theta \leq 80^{\circ}$  using Cu  $k\alpha$  radiation (40 kV, 40 mA). From the band intensity on  
32 the XRD analysis of the calcined dolomite, a composition of 32 % CaO and 67 % MgO  
33 was estimated. Surface areas of dolomite samples were measured by the Brunauer-  
34 Emmett-Teller (BET)  $\text{N}_2$  adsorption method at -196  $^{\circ}\text{C}$  using a *Micromeritics ASAP 2020*  
35 instrument.

36  $\text{H}_2$  temperature-programmed reduction (TPR) was performed on a *Micromeritics*  
37 *AutoChem II 2920* to analyze the reducibility of the Fe-metal species. The dolomite  
38 sample was firstly degassed at 200  $^{\circ}\text{C}$  and subsequently heated under reducing  
39 atmosphere (10 % vol.  $\text{H}_2$ -He) from 50  $^{\circ}\text{C}$  to 900  $^{\circ}\text{C}$  at 5  $^{\circ}\text{C}/\text{min}$ . The total amount of Fe  
40 impurities on the calcined dolomite (1074  $\mu\text{g}/\text{g}$ ) was measured by ICP-MS.

## 41 **2.3. Reaction equipment and operating conditions**

1 Schematic diagram of the reaction equipment used for the raw bio-oil upgrading  
2 experiments is shown in Fig. 1. The reactor consisted of a U-shaped stainless steel tube  
3 (1.6 cm inner diameter and 15 cm length) which was externally heated by an electric  
4 furnace. The 15 cm of pre-heating section (inlet side) allowed volatilization of the bio-oil  
5 prior to the catalytic section (outlet side), where the calcined dolomite was held by quartz  
6 wool above and below the bed. The carbonaceous solid, called pyrolytic lignin (PL) [33],  
7 was formed by re-polymerization of bio-oil compounds inside the pre-heater section. The  
8 resulting volatile stream passed through the dolomite bed. The controlled deposition of  
9 pyrolytic lignin prior to the catalytic bed minimizes the operating problems and attenuates  
10 catalyst deactivation. The reactor configuration enables continuous operation and  
11 separate collection of gas, liquid (upgraded oil) and solid (PL) reaction products. The  
12 relevance of this continuous upgrading alternative also lies in the possibility of accurately  
13 measuring the evolution with time on stream of products yield/selectivity, and hence the  
14 catalyst deactivation.

#### 15 **FIGURE 1**

16 The raw bio-oil was fed as droplets (injected using a pump *Harvard Apparatus 22*)  
17 that were carried by an inert He gas flow. Prior to each upgrading experiment, the as-  
18 received natural dolomite was sieved at 90-150  $\mu\text{m}$  range. Then it was activated by  
19 calcination at 850  $^{\circ}\text{C}$  for 5 h for obtaining CaO and MgO as active basic species.  
20 Additional water was fed (*307 Gilson* pump) in order to have a steam-to-carbon ratio of  
21 around 3. The experiments were carried out by feeding the raw bio-oil for 4 h at 400  $^{\circ}\text{C}$   
22 and 500  $^{\circ}\text{C}$  with a space-time of 2.8  $\text{g}_{\text{dolomite}}/\text{h}/\text{g}_{\text{bio-oil}}$ .

#### 23 **2.4. Reaction products characterization**

24 The volatile products stream was analyzed by on-line gas chromatograph (*Agilent*  
25 *Micro GC490*) provided with four analytical modules: i) 5A MS column for quantifying  
26  $\text{H}_2$ , CO, and  $\text{CH}_4$ ; ii) PPQ column for light oxygenates ( $\text{C}_2\text{-C}_4$ ),  $\text{CO}_2$  and  $\text{H}_2\text{O}$ ; iii) CPSil  
27 column for  $\text{C}_{5+}$  hydrocarbons; iv) Stabilwax column for  $\text{C}_{2+}$  oxygenated compounds.  
28 Furthermore, the volatile stream was sent to a condensation system (Peltier cell at 0  $^{\circ}\text{C}$ )  
29 and separated into condensable and non-condensable fractions (Fig. 1). The condensable  
30 fraction was obtained as a heterogeneous liquid with two different phases (aqueous and  
31 organic) that could be separated by decantation. The composition of the liquid collected  
32 throughout reaction (upgraded bio-oil) was analyzed by GC/MS (*Shimadzu QP2010S*  
33 device). The elemental analysis of the solid product deposited in the pre-heater section  
34 (pyrolytic lignin) was performed in a *EuroVector EA3000* Elemental Analyzer (CHNS).

35

#### 36 **2.5. Quantification of product yields**

37 The relative carbon yield in the gas, liquid and solid (PL) product was quantified on  
38 the basis of the carbon fed in the raw bio-oil, by using the carbon mass balances (overall  
39 carbon closure above 95 %) and according to the following equations:

$$1 \quad \text{Gas yield (C \%)} = \frac{F_{\text{Gas}}}{F_{\text{bio-oil}}} \times 100 \quad (1)$$

$$2 \quad \text{Liquid yield (C \%)} = \frac{F_{\text{Liq}}}{F_{\text{bio-oil}}} \times 100 \quad (2)$$

$$3 \quad \text{PL yield (C \%)} = \frac{m_{\text{PL}}}{F_{\text{bio-oil}}} \times 100 \quad (3)$$

4 where  $F_{\text{bio-oil}}$ ,  $F_{\text{gas}}$ , and  $F_{\text{liq}}$  is the carbon mass-flow (mg C/min) in the raw bio-oil, the gas,  
5 and the liquid product, respectively. The  $m_{\text{PL}}$  term is the rate of carbon deposition in the  
6 pyrolytic lignin (mg C/min), assuming linear deposition throughout reaction. The carbon  
7 yield in dolomite quantified the amount of the C fed in the raw bio-oil that was captured  
8 by the dolomite (resulting in  $\text{CaCO}_3$  formation by  $\text{CO}_2$  adsorption) and it was estimated  
9 by difference:

$$10 \quad C_{\text{dolomite}} \text{ (C \%)} = 100 - \text{Gas yield} - \text{Liquid yield} - \text{Solid yield} \quad (4)$$

11 Reporting the results in terms of carbon yield of individual products allows for tracking  
12 the fate of the carbon fed in the raw bio-oil. Recently, Saraeian et al. [34] emphasized the  
13 relevance of calculating the product yields in terms of overall mass and/or relative to the  
14 carbon in the feed for recognizing effective systems, strategies and catalysts for bio-oil  
15 upgrading. This would allow comparing small-scale and large-scale studies, as well as  
16 studies using different catalysts.

### 17 3. RESULTS AND DISCUSSION

#### 18 3.1. Activation of dolomite by calcination

19 The thermogravimetric TG (weight loss, %) and DTG (derivative weight loss, %/min)  
20 profiles resulting from thermal decomposition of the natural dolomite are depicted in Fig.  
21 2. It is observed that decomposition of this dolomite takes place in the 570–800 °C range,  
22 which is ascribed to direct transformation into the corresponding Ca and Mg oxides Eq.  
23 (5). The results indicate that the highest weight loss during the thermal decomposition  
24 occurs at 770 °C (single peak in DTG profile), and there is no weight loss above 800 °C.



#### 26 **FIGURE 2**

27 The X-ray diffraction pattern of the as-received dolomite is compared with that of  
28 activated dolomite in Fig. 3a. These results reveal a different crystalline structure of the  
29 natural and the calcined dolomite. The XRD of natural dolomite shows intense peaks at  
30  $2\theta = 30.9^\circ/33.6^\circ/35.4^\circ/37.4^\circ$  which correspond to  $\text{CaMg}(\text{CO}_3)_2$ , and peaks at  $2\theta =$   
31  $41.2^\circ/50.6^\circ/51.1^\circ$  corresponding to calcium peroxide ( $\text{CaO}_2$ ). Less intense peaks at  $2\theta =$

1 70.6°/72.9° corresponding to CaCO<sub>3</sub> are also detected. Accordingly, the natural dolomite  
2 is mainly composed of CaMg(CO<sub>3</sub>)<sub>2</sub>, and low amounts of CaO<sub>2</sub> and CaCO<sub>3</sub>. The XRD  
3 pattern of activated dolomite shows the diffraction peaks ascribed to the presence of CaO  
4 ( $2\theta = 32.5^\circ/37.6^\circ/54.1^\circ/67.6^\circ$ ) and MgO ( $2\theta = 43.2^\circ/74.9^\circ$ ). Peaks corresponding to  
5 CaMg(CO<sub>3</sub>)<sub>2</sub> are not detected.

6 Although a suitable calcination temperature for converting CaCO<sub>3</sub> into CaO is usually  
7 around 800 °C, it depends on the CaCO<sub>3</sub> source. For example, the CaCO<sub>3</sub> in oyster shells  
8 is transformed into CaO at 700 °C, whereas for eggshell and clamshell this transformation  
9 occurs at 800 °C, and for lime mud (industrial waste from pulp and paper mills) the  
10 calcination temperature is around 1000 °C [15]. The TG/DTG and XRD results indicate  
11 that 850 °C is a suitable calcination temperature for activating the dolomite used in this  
12 work.

13 The reducibility of the metal species contained in the activated dolomite was  
14 qualitatively characterized by TPR (Fig. 3b), showing a single broad reduction peak in  
15 the 500-650 °C range. According to Di Felice et al. [19], this peak may be ascribed to the  
16 MgFe<sub>2</sub>O<sub>4</sub> → Fe<sub>3</sub>O<sub>4</sub>-Fe<sub>3-x</sub>Mg<sub>x</sub>O<sub>4</sub> transition. This means that the Fe<sup>3+</sup> contained in activated  
17 dolomite is susceptible to reduction into Fe<sup>2.5+</sup> (Fe<sub>3</sub>O<sub>4</sub>) when it is subjected to a reductive  
18 atmosphere.

### 19 **FIGURE 3**

20 The crystal size of CaO and MgO were determined by applying the Scherrer equation  
21 to the CaO peak ( $2\theta = 37.6^\circ$ ) and the MgO peak ( $2\theta = 43.2^\circ$ ), resulting in average particle  
22 sizes of 85 nm and 47 nm, respectively, which reveal the nanocrystalline nature of these  
23 phases. High calcination temperatures induce the Mg surface segregation, resulting in  
24 MgO nanocrystals dispersed over CaO particles [35].

25 Morphology of the activated dolomite is significantly different than that of natural  
26 dolomite, thus revealing that CO<sub>2</sub> release during the thermal decomposition of  
27 CaMg(CO<sub>3</sub>)<sub>2</sub> (leading to CaO and MgO formation) modifies not only the chemical  
28 composition but also the physical properties. Consequently, the activated dolomite has  
29 many orderly pores on the surface which form a more porous structure, resulting in a  
30 higher surface area ( $S_{\text{BET}} = 12.2 \text{ m}^2 \text{ g}^{-1}$ ) than that of natural dolomite ( $S_{\text{BET}} = 1.7 \text{ m}^2 \text{ g}^{-1}$ ).

### 31 **3.2. Catalytic performance of activated dolomite**

32 Given the complexity of the raw bio-oil constituent molecules (mainly levoglucosan,  
33 acids, ketones and phenolics), they may react on the dolomite catalyst *via* several  
34 reactions (decarbonylation, decarboxylation, cracking, reforming, ketonization,  
35 condensation, dehydrocyclization/aromatization, polymerization, etc), which depend on  
36 the nature of the active sites and on the reaction conditions. Although the capability of  
37 activated dolomite for capturing CO<sub>2</sub> by carbonation is clear [36], the main goal of this  
38 section is to delve into the dolomite catalytic behavior at low reaction temperatures ( $\leq$   
39 500 °C). For this purpose, the distribution and composition of the products are analyzed



1 in detail. Besides, a thorough discussion on the role that the dolomite basic sites have on  
2 its catalytic behavior is presented below.

### 3 **3.2.1. Distribution of product yields**

4 Fig. 4 shows the evolution with time on stream of the relative C yield in solid (pyrolytic  
5 lignin), liquid (upgraded bio-oil) and gas (Eqs. (1)-(3)) for a reaction temperature of 400  
6 °C (Graph a) and 500 °C (Graph b). The yield denoted as “C in dolomite” quantifies the  
7 amount of carbon coming from the raw bio-oil which is “captured” (as adsorbed CO<sub>2</sub> to  
8 form CaCO<sub>3</sub> and as coke).

9 According to these results, liquid and solid are the majority products at 400 °C (Fig.  
10 4a) and the distribution of product yields changes notably by raising the temperature up  
11 to 500 °C. The gas yield increases, the liquid yield slightly decreases, whereas the  
12 deposition of pyrolytic lignin is significantly attenuated. Besides, the C yield in the  
13 dolomite is higher at 500 °C, which suggests enhancement of bio-oil decarboxylation  
14 reactions leading to the formation of CO<sub>2</sub>, which is subsequently absorbed by the  
15 dolomite.

#### 16 **FIGURE 4**

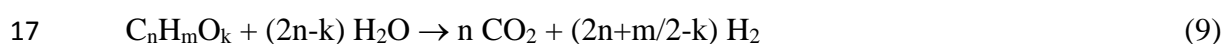
17 The different stages discerned in the evolution of the relative C yields (Fig. 4) are  
18 mainly attributed to the extent of the dolomite carbonation. For both temperatures, the C-  
19 yield in dolomite is highest at zero time on stream, owing to the greatest carbonation  
20 activity of the fresh dolomite. Besides, the initial C-yield in dolomite is higher at 500 °C  
21 (Fig. 4b) compared with 400 °C (Fig. 4a), which is explained by the greater extent of the  
22 bio-oil decarboxylation and ketonization reactions at this temperature. Consequently, a  
23 higher amount of C in the feed is converted into CO<sub>2</sub> that is captured by the dolomite.  
24 The carbonation of dolomite lasts approximately 2.3 h at 400 °C (Fig. 4a) and 2.7 h at  
25 500 °C (Fig. 4b). At 400 °C, the CO<sub>2</sub> capture capability of the dolomite progressively  
26 decreases, leading to a higher C yield in the gas product. At 500 °C, the gas yield remains  
27 practically steady for 1.8 h, after which there is a sharp increase indicating saturation of  
28 CO<sub>2</sub> capture capability. After complete carbonation of the dolomite, the gas and liquid  
29 yields remain almost steady until the end of the experiment. For both temperatures, the  
30 C-yield in the solid product (pyrolytic lignin, Fig. 1) is constant because a linear  
31 deposition was assumed throughout each reaction.

32 In order to properly explain the distribution of products (Fig. 4) and their composition  
33 (discussed in the following sections), different reactions must be taken into account in the  
34 catalytic activity of dolomite. In addition to CaO and MgO, the hydration of CaO leading  
35 to the formation of Ca(OH)<sub>2</sub> [37, 38] occurs during the bio-oil upgrading experiments  
36 (Eq. (7)). Given its exothermic nature, this reaction is more favored at 400 °C than at 500  
37 °C. It should be pointed out that this fact was experimentally evidenced by a sudden  
38 temperature increase ( $\approx 50$  °C) at the beginning of the experiment at 400 °C. The high  
39 basicity of the Ca(OH)<sub>2</sub> is likely to have an important role in dolomite activity for bio-oil  
40 oxygenates conversion.



4 Both CaO and the Ca(OH)<sub>2</sub> formed (which is also active for CO<sub>2</sub> capture, Eq. (8))  
5 deactivate during the experiments due to carbonation reaction. The relationship between  
6 Eq. (6) and Eq. (7) also suggests that the progressive CaO carbonation involves the  
7 Ca(OH)<sub>2</sub> disappearance.

8 Owing to the dolomite activity for bio-oil steam reforming [31, 39], both the  
9 oxygenates reforming, Eq. (9), and the water-gas-shift (WGS) reaction, Eq. (10), should  
10 also be considered, although they contribute to a moderate extent in the temperature range  
11 studied (400-500 °C). Considering the dolomite activity for cracking tar and long-chain  
12 hydrocarbons in biomass pyrolysis and gasification processes [18-21], the cracking  
13 reactions involving bio-oil oxygenates should be also taken into account. These reactions  
14 lead to the formation of CO, CO<sub>2</sub>, CH<sub>4</sub>, H<sub>2</sub> and light hydrocarbons. The CO<sub>2</sub> formation  
15 in steam reforming and cracking reactions would contribute to the extent of the CaO and  
16 Ca(OH)<sub>2</sub> carbonation (Eq. (6) and Eq. (8), respectively).



19 The afore-shown results evidence that the catalytic behavior of activated dolomite is  
20 significantly affected by the reaction temperature. The continuous reaction system allows  
21 analyzing the evolution with time on stream of the gas and liquid products composition.  
22 This provides useful information on the influence that the dolomite deactivation (by  
23 carbonation and coke deposition) has on its catalytic behavior, and allows to ascertain  
24 the prevailing reaction pathways. In the following sections, the composition of the gas  
25 product and the upgraded bio-oil are thoroughly analyzed and related with the catalytic  
26 behavior of the dolomite.

### 27 **3.2.2. Gas product composition**

28 The evolution with time on stream of the gas product composition (mol %) is shown  
29 in Fig. 5 at 400 °C (graph a) and 500 °C (graph b). The results reveal that CO<sub>2</sub> is effectively  
30 captured for more than 1.5 h at both temperatures, as well as a noticeable change in gas  
31 composition after dolomite saturation at 500 °C, due to the sharp increase in CO<sub>2</sub>  
32 concentration (Fig. 5b).

#### 33 **FIGURE 5**

34 Owing to the effective capture of CO<sub>2</sub> at 400°C, the gas produced is initially composed  
35 of 75 % H<sub>2</sub> and lower concentrations of CO (10 %), CH<sub>4</sub> (10 %), and C<sub>2</sub>-C<sub>4</sub> hydrocarbons  
36 (5 %). Then, the H<sub>2</sub> concentration decreases significantly throughout the carbonation  
37 period (≈ 1.5 h) and the CO, CH<sub>4</sub> and HCs concentration increase up to 40 %, 20 %, and  
38 10 %, respectively. This evolution on the gas composition is caused by the lower extent

1 of oxygenates reforming and WGS reaction (Eqs. (8)-(9)), as they are selectively  
2 deactivated thus promoting cracking reactions leading to CH<sub>4</sub> and HCs formation. Indeed,  
3 the significant content of CH<sub>4</sub> and C<sub>2</sub>-C<sub>4</sub> hydrocarbons is consistent with the reported  
4 cracking activity of dolomite in biomass catalytic pyrolysis and tar elimination processes  
5 [14, 21, 23]. The CO<sub>2</sub> concentration remains at negligible levels throughout the  
6 carbonation period, and then it increases until complete dolomite saturation ( $\approx$  2.5 h).

7 Although the initial H<sub>2</sub> concentration in the gas obtained at 500 °C is lower (55 %), the  
8 H<sub>2</sub> yield is higher due to the greater extent of oxygenates reforming and cracking reactions  
9 at this temperature, which lead to a higher total gas yield (Fig. 4). In the first hour of  
10 reaction, the H<sub>2</sub> concentration decreases from 55 % to 40 %, the CO increases from 20 %  
11 to 40 %, and the CH<sub>4</sub> and HCs concentration remain almost steady. The CO<sub>2</sub>  
12 concentration is negligible for 2 h and it becomes significant after dolomite saturation by  
13 carbonation, increasing sharply until a steady value. Consequently, the concentration of  
14 H<sub>2</sub>, CO, CH<sub>4</sub> and HCs decrease in the gas product.

### 15 **3.2.3. Liquid product composition**

16 The distribution of primary and trace compounds in the upgraded bio-oil collected  
17 throughout each experiment is shown in Table 1 (400 °C) and Table 2 (500 °C). The  
18 composition of the raw bio-oil and the liquid collected in experiments without dolomite  
19 (thermal treatment) are also shown in order to discern the catalytic effect. For both  
20 temperatures, the thermal treatment of raw bio-oil produces a bio-oil with acetic acid,  
21 acetol (1-hydroxy-2-propanone) and levoglucosan as majority compounds. It should be  
22 noted that this treated bio-oil has lower concentration of phenols but greater content of  
23 acids compared with the raw bio-oil

24 **TABLE 1**

25 **TABLE 2**

26 The results evidence that acids are completely removed, and phenols are partially  
27 converted when activated dolomite is used as upgrading catalyst. Other attractive feature  
28 of the upgraded bio-oil collected after short reaction time (0.5 h) is its high content of  
29 ketones, mainly acetone (26 % at 400 °C and 37 % at 500 °C), 2-butanone (11-19 %) and  
30 cyclopentanones (17-30 %). This result suggests that the dolomite has great activity for  
31 ketonization of bio-oil oxygenates, through pathways similar to those proposed using a  
32 wide variety of catalysts for upgrading pyrolysis oils [27, 29, 30, 40]. Also noteworthy is  
33 the presence of 7.3 % of aliphatic hydrocarbons (composed of linear C<sub>6</sub>-C<sub>12</sub> alkenes and  
34 C<sub>8</sub> cycloalkenes) in the upgraded bio-oil obtained at 500 °C.

35 Furthermore, the oxygenated phenols (i.e., guaiacols, catechols and heavy poly-  
36 substituted phenols) are completely eliminated from the raw bio-oil, with only phenol and  
37 alkyl-phenols being detected in the upgraded oil obtained throughout 0.5 h on stream.  
38 Several authors have reported the CaO activity for cracking aromatic ring side chains  
39 during catalytic pyrolysis of biomass at 450-600 °C [14, 41, 42]. The decrease in acids  
40 concentration is key to improve the bio-oil stability and reduce its corrosivity. It is also

1 desirable to decrease the high molecular weight phenols, given their tendency to  
2 polymerize and deactivate the catalyst in processes of bio-oil conversion into  
3 hydrocarbons [4, 5] and bio-oil steam reforming [6, 7]. Furthermore, the conversion of  
4 guaiacols (e.g. 2-methoxyphenol) and other oxygenated phenols (e.g. 4-hydroxy-3-  
5 methoxy-benzaldehyde) into alkyl-phenols contributes to decreasing the total oxygen  
6 content in the bio-oil.

7 The results in Table 1 and Table 2 show an increasing content of acids and phenols  
8 with time on stream (especially after dolomite saturation when CaO and Ca(OH)<sub>2</sub> are  
9 fully carbonated to CaCO<sub>3</sub>), as well as a decreasing concentration of ketones. Although  
10 the alkyl-phenols still remain as majority compounds, the content of guaiacols and  
11 catechols become significant after 4 h reaction. This result is consistent with preliminary  
12 remarks on dolomite activity [31], and confirms that guaiacol demethylation/dehydration  
13 pathway is enhanced as dolomite deactivates. This may also contribute to the high  
14 concentration of CH<sub>4</sub> observed in gas product (Fig. 5).

15 The aforementioned results reveal that the raw bio-oil upgrading with activated  
16 dolomite takes place through different reaction pathways, due to the different catalytic  
17 role of CaO, MgO and Ca(OH)<sub>2</sub> basic oxides, and the acid CaCO<sub>3</sub> resulting from  
18 carbonation. The prevailing reaction pathways under the operating conditions used (low  
19 temperature  $\leq 500$  °C and high water content) will be proposed and discussed in Section  
20 3.3.

#### 21 **3.2.4. Characteristics of deactivated dolomite**

22 The X-ray diffraction analysis of fresh catalyst (activated dolomite) is compared with  
23 those corresponding to dolomite after reaction at 400 °C and 500 °C (Fig. 6). The XRD  
24 patterns reveal that fresh dolomite is composed of CaO and MgO. The presence of CaO  
25 is not detected in any of the deactivated dolomite samples, which are mainly composed  
26 of CaCO<sub>3</sub> and MgO. These results evidence that all the CaO contained in dolomite is  
27 carbonated to CaCO<sub>3</sub> during the experiments, whereas the Mg remains in oxide phase  
28 (MgO).

29 The presence of residual Ca(OH)<sub>2</sub> ( $2\theta = 18.3/34.2$ ) is detected both in the dolomite  
30 deactivated at 500 °C ( $\approx 5$  %) and at 400 °C ( $\approx 1$  %), which can be explained by the  
31 thermodynamics of the Ca(OH)<sub>2</sub> carbonation (Eq. 8). Given the exothermic nature of this  
32 reaction, Ca(OH)<sub>2</sub> carbonation is more favored at 400 °C than at 500 °C. Furthermore, the  
33 absence of MgCO<sub>3</sub> confirms the fact that the MgO contained in dolomite does not  
34 contribute to the carbonation reaction under the operating conditions studied [14].

35 As discussed in Section 3.2.1, the C "retained" in the deactivated dolomite (C-yield  
36 shown in Fig. 4) includes the CO<sub>2</sub> adsorbed (to form CaCO<sub>3</sub>) and the coke deposited. Fig.  
37 7 depicts the weight loss and the CO<sub>2</sub> signal recorded during the calcination-combustion  
38 TG analysis (described in Section 2.2), which allows to discern between the C coming  
39 from carbonation and that corresponding to the coke. The first peak is ascribed to the CO<sub>2</sub>  
40 captured by the dolomite, which is released during the calcination stage. The second peak  
41 corresponds to the CO<sub>2</sub> produced by combustion of the coke deposited. From these

1 results, both the amount of C adsorbed and the coke deposited on the deactivated dolomite  
2 are quantified (Table 3).

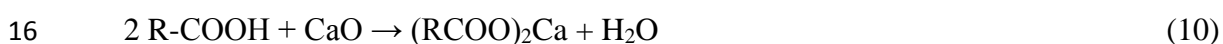
3 **FIGURE 6**

4 **FIGURE 7**

5 **TABLE 3**

### 6 **3.3. Reaction pathways in raw bio-oil upgrading**

7 The absence of acetic acid, as well as the high content of acetone in the upgraded bio-  
8 oil collected throughout 0.5 h (Table 1 and Table 2) clearly indicate the dolomite activity  
9 for acetic acid ketonization. Similarly, ketonization reactions involving other carboxylic  
10 acids may occur leading to the formation of linear ketones. It is well-established in the  
11 literature that acids can be converted through three reaction pathways: neutralization,  
12 thermal cracking and catalytic cracking. As previously reported, acids can react with CaO  
13 by neutralization reaction to form calcium carboxylate and H<sub>2</sub>O, Eq. (10) [38, 43].  
14 Calcium carboxylate would decompose to ketones and CaCO<sub>3</sub> at the temperature range  
15 of 400–500 °C, Eq. (11) [44-46]:



18 Fig. 8. shows a scheme that gathers ketonization and other possible reaction pathways  
19 involved in the raw bio-oil conversion with activated dolomite under the operating  
20 conditions used (high water content and temperatures  $\leq 500$  °C). In addition to coming  
21 from carboxylic acids, acetone and 2-butanone could be also produced from acetol (1-  
22 hydroxy-2-propanone) *via* the intermediates acetic acid (which undergoes ketonization)  
23 and propanal (which undergoes carbonylation, hydrogenation, and dehydration) [27, 29].  
24 Apparently, these are the prevailing reactions promoted by the activated dolomite, which  
25 lead to the formation of acetone and 2-butanone (the main linear ketones detected in the  
26 upgraded bio-oil). Moreover, the selectivity to linear ketones is increased by raising  
27 temperature from 400 °C to 500 °C.

28 The high content of cyclopentanone and alkyl-substituted cyclopentanones in the  
29 upgraded bio-oil produced throughout 0.5 h on stream (C5-ring ketones, Table 1 and  
30 Table 2) is an outstanding result, as they are interesting raw materials in medicine,  
31 pesticide and fragrance industries. The significant formation of cyclic ketones can be  
32 explained by the transformation of anhydrosugars (mainly levoglucosan) *via*  
33 rearrangement reactions of furfuryl type compounds (e.g., furfural) [47] (Fig. 8). It should  
34 be noted that these reactions are promoted by the high concentration of water in the  
35 reaction medium [29, 48, 49], and also by the H<sub>2</sub> coming from the dolomite activity for  
36 SR and WGS reactions (Eqs.(9)-(10)). Another possible pathway of forming  
37 cyclopentanone could be cyclo-ketonization of the adipic acid resulting from the catalytic

1 reduction of levoglucosan and other anhydrosugars [50, 51]. It should be pointed out that  
2 this reaction is promoted by the presence of  $\text{Ca}(\text{OH})_2$ . Renz and Corma [52] reported a  
3 high activity of  $\text{Ca}(\text{OH})_2$  for adipic acid ketonization using a dry distillation method at  
4  $350\text{ }^\circ\text{C}$ . The formation of acetaldehyde (not detected in the raw bio-oil) suggests that this  
5 dolomite is also active for acetic acid hydrogenation to acetaldehyde, which could be  
6 attributed to the catalytic activity of the Fe impurities under a  $\text{H}_2$ -rich atmosphere [53].

7

### FIGURE 8

8 The decreasing content of ketones with time on stream in parallel to the increasing  
9 content of acids suggests dolomite deactivation, which is caused both by the  
10  $\text{CaO}/\text{Ca}(\text{OH})_2$  carbonation and by coke deposition. Indeed, the sharp increase in the  
11 content of phenols in the upgraded bio-oil obtained after  $\approx 4\text{ h}$  on stream at  $400\text{ }^\circ\text{C}$  (Table  
12 1) and after  $\approx 2\text{ h}$  at  $500\text{ }^\circ\text{C}$  (Table 2) can be directly related to the dolomite saturation  
13 (Fig. 4-5). This result suggests that  $\text{CaO}$  and  $\text{Ca}(\text{OH})_2$  basic oxides are the main active  
14 sites responsible for ketonization reactions, whereas the  $\text{CaCO}_3$  seems to be almost  
15 inactive. As these ketonization reactions deactivate, the reactions leading to phenols  
16 formation (mainly alkyl-phenols and catechols) become significant. These reactions,  
17 which are apparently activated by the  $\text{CaCO}_3$  and  $\text{MgO}$  contained in dolomite, seem to be  
18 enhanced by raising the temperature.

19 The results of this work are consistent with those obtained in previous studies on the  
20 *in-situ* catalytic pyrolysis of lignocellulosic biomass with calcined dolomite [23, 24], as  
21 well as on the catalytic upgrading of biomass pyrolysis vapors over  $\text{CaO}$  and  $\text{MgO}$  based  
22 catalysts using an analytical pyrolysis-gas chromatography/mass spectrometry system  
23 (Py-GC/MS) [41, 54, 55]. Ly et al. [23] state that dolomite changes the composition of  
24 the bio-oil obtained by pyrolysis of tulip tree at  $450\text{ }^\circ\text{C}$  by reducing significantly the  
25 content of levoglucosan and promoting the formation of ketones (mainly  
26 cyclopentenones) and phenolic compounds. The decrease in levoglucosan is attributed to  
27 the ring-breaking reactions promoted by the Ca and Mg contained in dolomite. Lu et al.  
28 [41] compare the catalytic behavior of  $\text{CaO}$ ,  $\text{MgO}$  and  $\text{Fe}_2\text{O}_3$  and conclude that  $\text{CaO}$   
29 decreases the levoglucosan content and fully eliminates acids, while greatly promoting  
30 the formation of linear ketones and cyclopentanones. Conversely,  $\text{MgO}$  and  $\text{Fe}_2\text{O}_3$  result  
31 in higher formation of phenols and aromatic compounds but they are not able to reduce  
32 the acids.

33 It should be highlighted that ketonization of real bio-oil has been scarcely studied in  
34 the literature. A simulated bio-oil consisting of acetic acid, acetol, and furfural has been  
35 upgraded by Hakim et al. [27] in a continuous flow reactor using  $\text{CeZrO}_x$  as a catalyst.  
36 Although the acetic acid content is significantly reduced, they have found that the  
37 presence of furfural decreases the ketonization activity. A more realistic study has been  
38 conducted by Mansur et al. [28] upgrading the water-soluble fraction of a bio-oil  
39 (obtained by slow pyrolysis of cedar woodchips) with zirconia-supported iron-oxides  
40 ( $\text{ZrO}_2\text{-FeO}_x$ ) at  $350\text{-}450\text{ }^\circ\text{C}$ . Similar to our results, they report that hydroxyacetone and  
41 carboxylic acids (acetic and propionic acids) are converted into ketones (acetone and 2-

1 butanone). More recently, Kastner and co-workers [29, 30] have used a continuous  
2 packed bed reactor for upgrading a water extracted bio-oil over iron oxide catalysts  
3 derived from red mud. These authors also report that acetol and carboxylic acids are  
4 primarily converted into acetone and 2-butanone, with the highest yield being produced  
5 at relatively low temperatures (350-500 °C).

## 6 CONCLUSIONS

7 Natural dolomite has been successfully activated and applied to raw bio-oil continuous  
8 upgrading process by means of a reaction system that enables separate collection and  
9 analysis of reaction products. This allowed studying the evolution with time on stream of  
10 the upgraded bio-oil composition. The activated dolomite is capable of removing  
11 carboxylic acids, acetol (1-hydroxy-2-propanone) and anhydrosugars (levoglucosan)  
12 from the bio-oil, whereas the formation of linear ketones (acetone and 2-butanone) and  
13 cyclopentanones is greatly increased. The heavy oxygenated phenols (e.g., guaiacols,  
14 catechols and poly-substituted phenols) are also converted into light alkyl-phenols by  
15 removing the methoxyl and hydroxyl groups.

16 The dolomite activity for ketonization, water-gas-shift, steam reforming and cracking  
17 reactions is attributed to its basic nature, due to the presence of CaO/MgO basic oxides  
18 and strongly basic Ca(OH)<sub>2</sub>. Under the upgrading conditions used (high water content  
19 and temperatures  $\leq 500$  °C), the basic sites of activated dolomite promote acetic acid and  
20 levoglucosan conversion *via* ketonization reactions. The steam reforming and water-gas-  
21 shift reactions are enhanced by dolomite capability for CO<sub>2</sub> capture. As dolomite  
22 deactivates (by carbonatation of Ca(OH)<sub>2</sub> and CaO to CaCO<sub>3</sub> and by coke deposition),  
23 cracking reactions involving poly-substituted phenols that lead to the formation of alkyl-  
24 phenols become significant. After 0.5 h on stream at 400 °C, 48 % of the carbon fed in  
25 the raw bio-oil is converted into a high-quality bio-oil with low corrosive nature  
26 (negligible acid content) and high concentration of linear ketones (37 % acetone + 2-  
27 butanone) and cyclopentanones (30 %).

28 Consequently, the development of this cost-effective continuous process (which uses  
29 low-cost dolomite as catalyst, operates at atmospheric pressure and without external H<sub>2</sub>  
30 supply) is of great interest with regard to carbon efficiency, and composition of the  
31 upgraded bio-oil for its downstream valorization for producing fuels, chemicals, and  
32 particularly, H<sub>2</sub> by steam reforming.

## 33 Acknowledgements

34 This work was carried out with the financial support of the Department of Education  
35 Universities and Investigation of the Basque Government (IT-748-13), the Ministry of  
36 Economy and Competitiveness of the Spanish Government jointly with European  
37 Regional Development Funds (AEI/FEDER, UE) (Project CTQ2015-68883-R), and PhD  
38 grant (BES-2016-078132) for N. García-Gómez.

## 39 REFERENCES

- 1 [1] A.N. Oumer, M.M. Hasan, A.T. Baheta, R. Mamat, A.A. Abdullah, Bio-based  
2 liquid fuels as a source of renewable energy: A review, *Renewable Sustainable*  
3 *Energy Rev.* 88 (2018) 82-98.
- 4 [2] B. Valle, A. Remiro, N. García-Gómez, A.G. Gayubo, J. Bilbao, Recent research  
5 progress on bio-oil conversion into bio-fuels and raw chemicals: a review, *J. Chem.*  
6 *Technol. Biotechnol.* 94 (2019) 670-689.
- 7 [3] J. Alvarez, M. Amutio, G. Lopez, M. Olazar, J. Bilbao, Chapter 6- Bio-oil  
8 production, in O. Konur (Ed.), *Bioenergy and Biofuels*, Taylor & Francis, Boca  
9 Raton, 2018.
- 10 [4] A.G. Gayubo, A.T. Aguayo, A. Atutxa, B. Valle, J. Bilbao, Undesired components  
11 in the transformation of biomass pyrolysis oil into hydrocarbons on an HZSM-5  
12 zeolite catalyst, *J. Chem. Technol. Biotechnol.* 80 (2005) 1244-1251.
- 13 [5] B. Valle, P. Castaño, M. Olazar, J. Bilbao, A.G. Gayubo, Deactivating species in  
14 the transformation of crude bio-oil with methanol into hydrocarbons on a HZSM-5  
15 catalyst, *J. Catal.* 285 (2012) 304-314.
- 16 [6] A. Ochoa, B. Aramburu, B. Valle, D.E. Resasco, J. Bilbao, A.G. Gayubo, P.  
17 Castano, Role of oxygenates and effect of operating conditions in the deactivation  
18 of a Ni supported catalyst during the steam reforming of bio-oil, *Green Chem.* 19  
19 (2017) 4315-4333.
- 20 [7] B. Valle, N. García-Gómez, A. Arandia, A. Remiro, J. Bilbao, A.G. Gayubo, Effect  
21 of phenols extraction on the behavior of Ni-spinel derived catalyst for raw bio-oil  
22 steam reforming, *Int. J. Hydrogen Energy* 44 (2019) 12593-12603.
- 23 [8] A. Oasmaa, I. Fonts, M.R. Pelaez-Samaniego, M.E. Garcia-Perez, M. Garcia-Perez,  
24 Pyrolysis oil multiphase behavior and phase stability: A review. *Energy Fuels* 30  
25 (2016) 6179-6200.
- 26 [9] J. Feroso, P. Pizarro, J.M. Coronado, D.P. Serrano, Advanced biofuels production  
27 by upgrading of pyrolysis bio-oil, *Wiley Interdiscip. Rev.: Energy Environ.* 6  
28 (2017) e245.
- 29 [10] P.M. Mortensen, J.D. Grunwaldt, P.A. Jensen, K.G. Knudsen, A.D. Jensen, A  
30 review of catalytic upgrading of bio-oil to engine fuels, *Appl. Catal., A* 407 (2011)  
31 1-19.
- 32 [11] A.H. Zacher, M.V. Olarte, D.M. Santosa, D.C. Elliott, S.B. Jones, A review and  
33 perspective of recent bio-oil hydrotreating research, *Green Chem.* 16 (2014) 491-  
34 515.
- 35 [12] S. Arbogast, D. Bellman, J.D. Paynter, J. Wykowski, Advanced bio-fuels from  
36 pyrolysis oil: The impact of economies of scale and use of existing logistic and  
37 processing capabilities, *Fuel Process. Technol.* 104 (2012) 121-127.
- 38 [13] S. Arbogast, D. Bellman, J.D. Paynter, J. Wykowski, Advanced biofuels from  
39 pyrolysis oil...Opportunities for cost reduction, *Fuel Process. Technol.* 106 (2013)  
40 518-525.
- 41 [14] A. Veses, M. Aznar, I. Martínez, J.D. Martínez, J.M. López, M.V. Navarro, M.S.  
42 Callén, R. Murillo, T. García, Catalytic pyrolysis of wood biomass in an auger  
43 reactor using calcium-based catalysts, *Bioresour. Technol.* 162 (2014) 250-258.



- 1 [15] S. Vichaphund, V. Sricharoenchaikul, D. Atong, Industrial waste derived CaO-  
2 based catalysts for upgrading volatiles during pyrolysis of Jatropha residues, J.  
3 Anal. Appl. Pyrolysis 124 (2017) 568-575.
- 4 [16] S.D. Stefanidis, S.A. Karakoulia, K.G. Kalogiannis, E.F. Iliopoulou, A. Delimitis,  
5 H. Yiannoulakis, T. Zampetakis, A.A. Lappas, K.S. Triantafyllidis, Natural  
6 magnesium oxide (MgO) catalysts: A cost-effective sustainable alternative to acid  
7 zeolites for the in situ upgrading of biomass fast pyrolysis oil, Appl. Catal., B 196  
8 (2016) 155-173.
- 9 [17] A. Orío, J. Corella, I. Narváez, Characterization and activity of different dolomites  
10 for hot gas cleaning in biomass gasification, in A.V. Bridgwater, D.G.B. Boocock  
11 (Eds), *Developments in Thermochemical Biomass Conversion*, Springer,  
12 Dordrecht, 1997, pp 1144-1157.
- 13 [18] L. Devi, K.J. Ptasiński, F.J.J.G. Janssen, S.V.B. van Paasen, P.C.A. Bergman,  
14 J.H.A. Kiel, Catalytic decomposition of biomass tars: use of dolomite and untreated  
15 olivine, *Renewable Energy* 30 (2005) 565-587.
- 16 [19] L. Di Felice, C. Courson, D. Niznansky, P.U. Foscolo, A. Kiennemann, Biomass  
17 gasification with catalytic tar reforming: A model study into activity enhancement  
18 of calcium- and magnesium-oxide-based catalytic materials by incorporation of  
19 iron, *Energy Fuels* 24 (2010) 4034-4045.
- 20 [20] J. Corella, J.M. Toledo, R. Padilla, Olivine or dolomite as in-bed additive in  
21 biomass gasification with air in a fluidized bed: Which is better? *Energy Fuels* 18  
22 (2004) 713-720.
- 23 [21] C. Berrueco, D. Montané, B. Matas Güell, G. del Alamo, Effect of temperature and  
24 dolomite on tar formation during gasification of torrefied biomass in a pressurized  
25 fluidized bed, *Energy* 66 (2014) 849-859.
- 26 [22] R. Li, Z.P. Zhong, B.S. Jin, A.J. Zheng, Application of mineral bed materials during  
27 fast pyrolysis of rice husk to improve water-soluble organics production, *Bioresour.*  
28 *Technol.* 119 (2012) 324-330.
- 29 [23] H.V. Ly, D.-H. Lim, J.W. Sim, S.-S. Kim, J. Kim, Catalytic pyrolysis of tulip tree  
30 (*Liriodendron*) in bubbling fluidized-bed reactor for upgrading bio-oil using  
31 dolomite catalyst, *Energy* 162,(2018) 564-575.
- 32 [24] W. Charusiri, T. Vitidsant, Upgrading bio-oil produced from the catalytic pyrolysis  
33 of sugarcane (*Saccharum officinarum* L) straw using calcined dolomite, *Sustainable*  
34 *Chem. Pharm.* 6 (2017) 114-123.
- 35 [25] M. Glinski, J. Kijenski, A. Jakubowski, Ketones from monocarboxylic acids:  
36 Catalytic ketonization over oxide systems, *Appl. Catal., A* 128 (1995) 209-217.
- 37 [26] T.N. Pham, D. Shi, D.E. Resasco, Evaluating strategies for catalytic upgrading of  
38 pyrolysis oil in liquid phase, *Appl. Catal., B* 145 (2014) 10-23.
- 39 [27] S.H. Hakim, B.H. Shanks, J.A. Dumesic, Catalytic upgrading of the light fraction  
40 of a simulated bio-oil over CeZrO<sub>x</sub> catalyst, *Appl. Catal., B* 142-143 (2013) 368-  
41 376.
- 42 [28] D. Mansur, T. Yoshikawa, K. Norinaga, J.-I. Hayashi, T. Tago, T. Masuda,  
43 Production of ketones from pyroligneous acid of woody biomass pyrolysis over an  
44 iron-oxide catalyst, *Fuel* 103 (2013) 130-134.

- 1 [29] J.R. Kastner, R. Hilten, J. Weber, A.R. McFarlane, J.S.J. Hargreaves, V.S. Batra,  
2 Continuous catalytic upgrading of fast pyrolysis oil using iron oxides in red mud,  
3 RSC Advances 5 (2015) 29375-29385.
- 4 [30] J. Weber, A. Thompson, J. Wilmoth, V.S. Batra, N. Janulaitis, J.R. Kastner, Effect  
5 of metal oxide redox state in red mud catalysts on ketonization of fast pyrolysis oil  
6 derived oxygenates, Appl. Catal., B 241 (2019) 430-441.
- 7 [31] B. Valle, B. Aramburu, C. Santiviago, J. Bilbao, A.G. Gayubo, Upgrading of bio-  
8 oil in a continuous process with dolomite catalyst, Energy Fuels 28 (2014) 6419-  
9 6428.
- 10 [32] M. Garcia-Perez, A. Chala, H. Pakdel, D. Kretschmer, C. Roy, Characterization  
11 of bio-oils in chemical families, Biomass Bioenergy 31 (2007) 222-242.
- 12 [33] A. Ochoa, B. Aramburu, M. Ibáñez, B. Valle, J. Bilbao, A.G. Gayubo, P. Castaño,  
13 Compositional insights and valorization pathways for carbonaceous material  
14 deposited during bio-oil thermal treatment, ChemSusChem 7 (2014) 2597-2608.
- 15 [34] A. Saraeian, M.W. Nolte, B.H. Shanks, Deoxygenation of biomass pyrolysis  
16 vapors: Improving clarity on the fate of carbon, Renewable Sustainable Energy  
17 Rev. 104 (2019) 262-280.
- 18 [35] A.F. Lee, K. Wilson, Recent developments in heterogeneous catalysis for the  
19 sustainable production of biodiesel, Catal. Today 242 (2015) 3-18.
- 20 [36] A. Remiro, B. Valle, B. Aramburu, A.T. Aguayo, J. Bilbao, A.G. Gayubo, Steam  
21 reforming of the bio-oil aqueous fraction in a fluidized bed reactor with in situ CO<sub>2</sub>  
22 capture, Ind. Eng. Chem. Res. 52 (2013) 17087-17098.
- 23 [37] H.W. Lee, Y.-M. Kim, J. Jae, S.M. Lee, S.-C. Jung, Y.-K. Park, The use of calcined  
24 seashell for the prevention of char foaming/agglomeration and the production of  
25 high-quality oil during the pyrolysis of lignin. Renew. Energy, In press,  
26 <https://doi.org/10.1016/j.renene.2018.07.093>.
- 27 [38] D. Wang, R. Xiao, H. Zhang, G. He, Comparison of catalytic pyrolysis of biomass  
28 with MCM-41 and CaO catalysts by using TGA-FTIR analysis, J. Anal. Appl.  
29 Pyrolysis 89 (2010) 171-177.
- 30 [39] B. Aramburu, B. Valle, C. Santiviago, J. Bilbao, A.G. Gayubo, Effect of  
31 temperature on the catalytic performance of dolomite for H<sub>2</sub> production by steam  
32 reforming of a bio-oil/ethanol mixture, Chem. Eng. Trans. 37 (2014) 6.
- 33 [40] E. Karimi, C. Briens, F. Berruti, S. Moloodi, T. Tzanetakis, M.J. Thomson, M.  
34 Schlaf, Red mud as a catalyst for the upgrading of hemp-seed pyrolysis bio-oil,  
35 Energy Fuels 24 (2010) 6586-6600.
- 36 [41] Q. Lu, Z.-F. Zhang, C.-Q. Dong, X.-F. Zhu, Catalytic upgrading of biomass fast  
37 pyrolysis vapors with nano metal oxides: An analytical Py-GC/MS study, Energies  
38 3 (2010) 1805-1820.
- 39 [42] Y. Lin, C. Zhang, M. Zhang, J. Zhang, Deoxygenation of bio-oil during pyrolysis  
40 of biomass in the presence of CaO in a fluidized-bed reactor, Energy Fuels 24  
41 (2010) 5686-5695.
- 42 [43] Y. Zheng, L. Tao, Y. Huang, C. Liu, Z. Wang, Z. Zheng, Improving aromatic  
43 hydrocarbon content from catalytic pyrolysis upgrading of biomass on a  
44 CaO/HZSM-5 dual-catalyst, J. Anal. Appl. Pyrolysis 140 (2019). 140, 355-366.

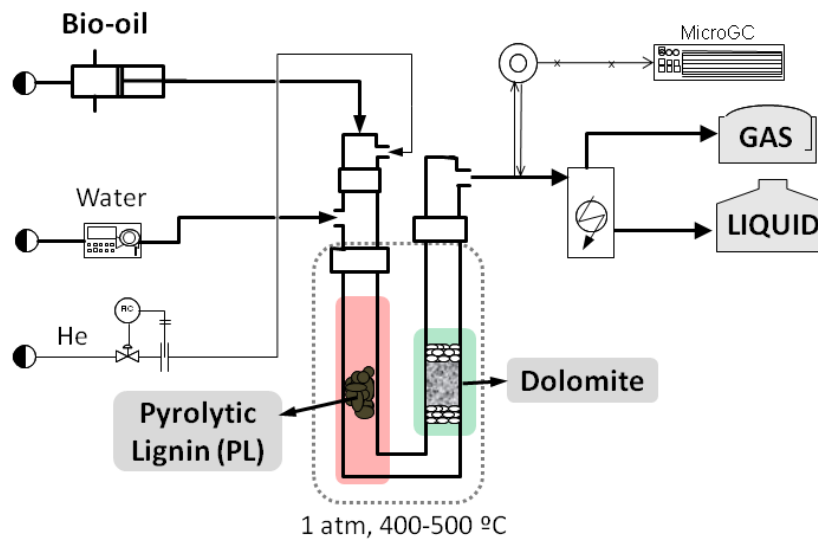
- 1 [44] L. Yi, H. Liu, K. Xiao, G. Wang, Q. Zhang, H. Hu, H. Yao, In situ upgrading of  
2 bio-oil via CaO catalyst derived from organic precursors, *Proc. Combust. Inst.* 37  
3 (2019) 3119-3126.
- 4 [45] H. Lu, A. Khan, P.G. Smirniotis, Relationship between structural properties and  
5 CO<sub>2</sub> capture performance of CaO-based sorbents obtained from different  
6 organometallic precursors. *Ind. Eng. Chem. Res.* 47 (2008) 6216-6220.
- 7 [46] X. Yang, J. Zhang, X. Zhu, Decomposition and calcination characteristics of  
8 calcium-enriched bio-oil, *Energy Fuels* 22 (2008) 2598-2603.
- 9 [47] M. Zhou, J. Li, K. Wang, H. Xia, J. Xu, J. Jiang, Selective conversion of furfural to  
10 cyclopentanone over CNT-supported Cu based catalysts: Model reaction for  
11 upgrading of bio-oil, *Fuel* 202 (2017) 1-11.
- 12 [48] M. Källdström, N. Kumar, T. Heikkilä, M. Tiitta, T. Salmi, D.Y. Murzin, Formation  
13 of furfural in catalytic transformation of levoglucosan over mesoporous materials,  
14 *ChemCatChem* 2 (2010) 539-546.
- 15 [49] M. Hronec, K. Fulajtarov, T. Liptaj, Effect of catalyst and solvent on the furan ring  
16 rearrangement to cyclopentanone, *Appl. Catal., A* 437-438 (2012) 104-111.
- 17 [50] F.H. Isikgor, C.R. Becer, Lignocellulosic biomass: a sustainable platform for the  
18 production of bio-based chemicals and polymers, *Polymer Chemistry* 6 (2015)  
19 4497-4559.
- 20 [51] K. Wilson, A.F. Lee, J.-P. Dacquin, Heterogeneous catalysts for converting  
21 renewable feedstocks to fuels and chemicals, In L. Guzzi, A. Erdöhelyi (Eds.)  
22 *Catalysis for Alternative Energy Generation*, Springer, New York, 2012, 263-304.
- 23 [52] M. Renz, A. Corma, Ketonic decarboxylation catalysed by weak bases and its  
24 application to an optically pure substrate, *Eur. J. Org. Chem.* 2004 (2004) 2036-  
25 2039.
- 26 [53] W. Rachmady, M.A. Vannice, Acetic acid reduction to acetaldehyde over iron  
27 catalysts: I. Kinetic behavior, *J. Catal.* 208 (2002) 158-169.
- 28 [54] X. Zhang, L. Sun, L. Chen, X. Xie, B. Zhao, H. Si, G. Meng, Comparison of  
29 catalytic upgrading of biomass fast pyrolysis vapors over CaO and Fe(III)/CaO  
30 catalysts, *J. Anal. Appl. Pyrolysis* 108 (2014) 35-40.
- 31 [55] L. Sun, X. Zhang, L. Chen, B. Zhao, S. Yang, X. Xie, Effects of Fe contents on fast  
32 pyrolysis of biomass with Fe/CaO catalysts, *J. Anal. Appl. Pyrolysis* 119 (2016)  
33 133-138.  
34

## 1 **FIGURE CAPTIONS**

- 2 **Figure 1.** Schematic diagram of the experimental equipment.
- 3 **Figure 2.** Thermogravimetric analysis of as-received natural dolomite.
- 4 **Figure 3.** Characteristics of dolomite: XRD of natural and activated dolomite (Graph a)  
5 and TPR of activated dolomite (Graph b).
- 6 **Figure 4.** Evolution with time on stream of carbon yields (C wt%) in dolomite, solid  
7 (pyrolytic lignin), liquid (upgraded bio-oil) and gas products. Reaction  
8 temperature: 400 °C (Graph a) and 500 °C (Graph b).
- 9 **Figure 5.** Evolution with time on stream of the gas product composition (mol %) at 400  
10 °C (Graph a) and 500 °C (Graph b).
- 11 **Figure 6.** XRD patterns of activated dolomite (a) and dolomite deactivated after  
12 reaction at 400 °C (b) and 500 °C (c).
- 13 **Figure 7.** Calcination-combustion TG-MS analyses of dolomite deactivated after 4 h  
14 reaction at 400 °C (a) and 500 °C (b).
- 15 **Figure 8.** Proposed reaction pathways for the conversion of bio-oil majority compounds  
16 over activated dolomite under upgrading conditions of high water content  
17 (S/C= 3) and low temperature ( $\leq 500$  °C).  
18

1

## FIGURES

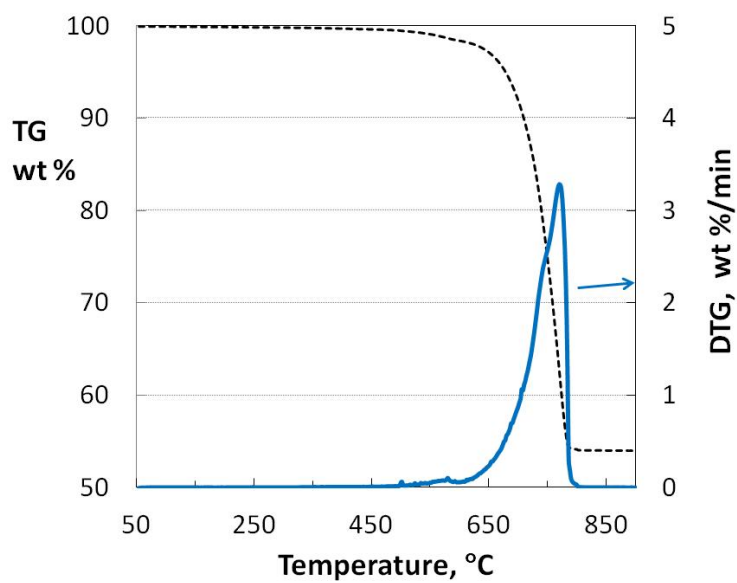


2

3

**Figure 1**

4



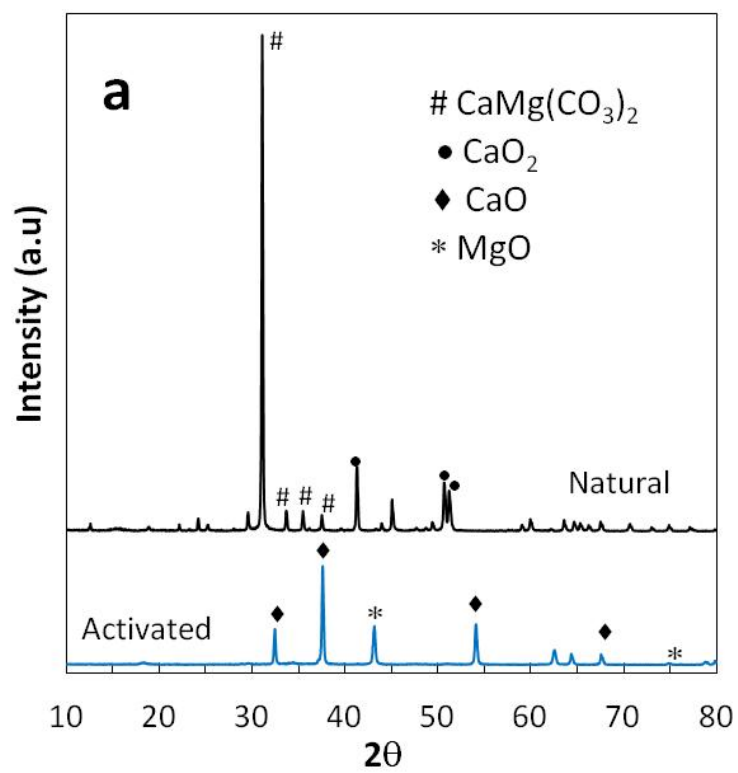
5

6

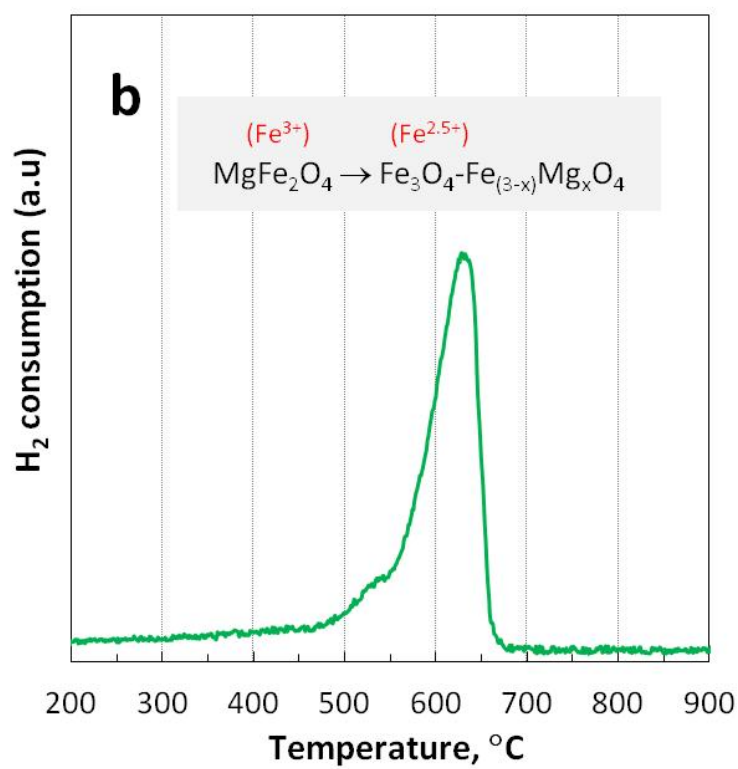
**Figure 2**

7

1



2

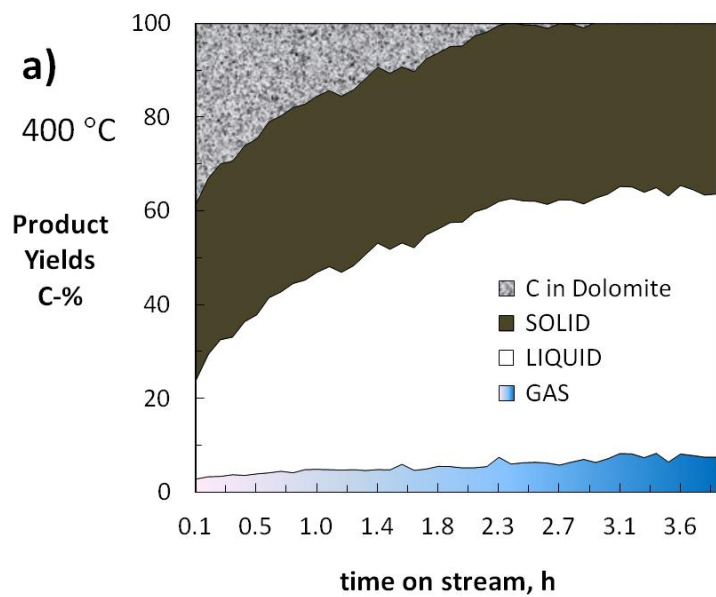


3

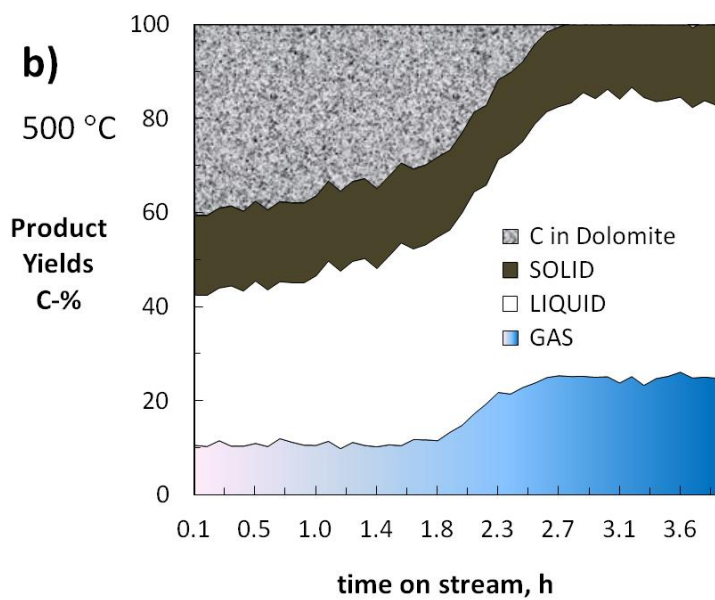
4

5

Figure 3



1

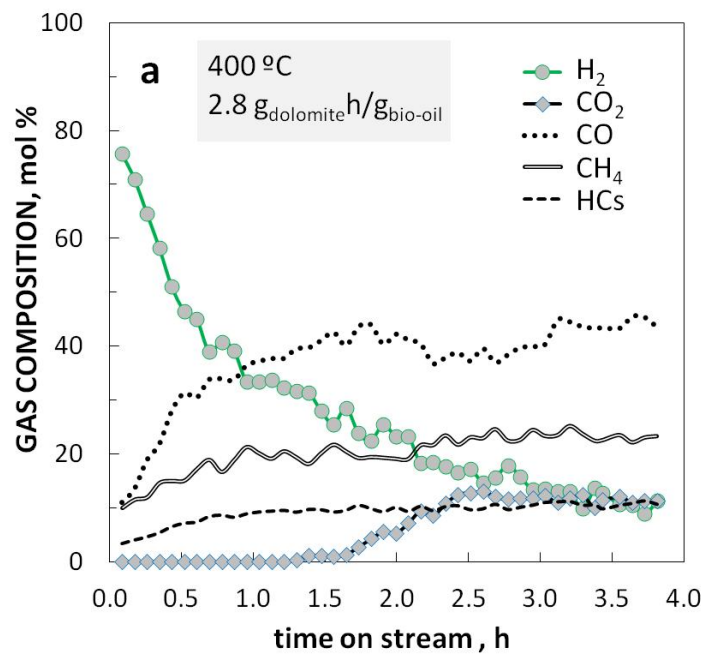


2

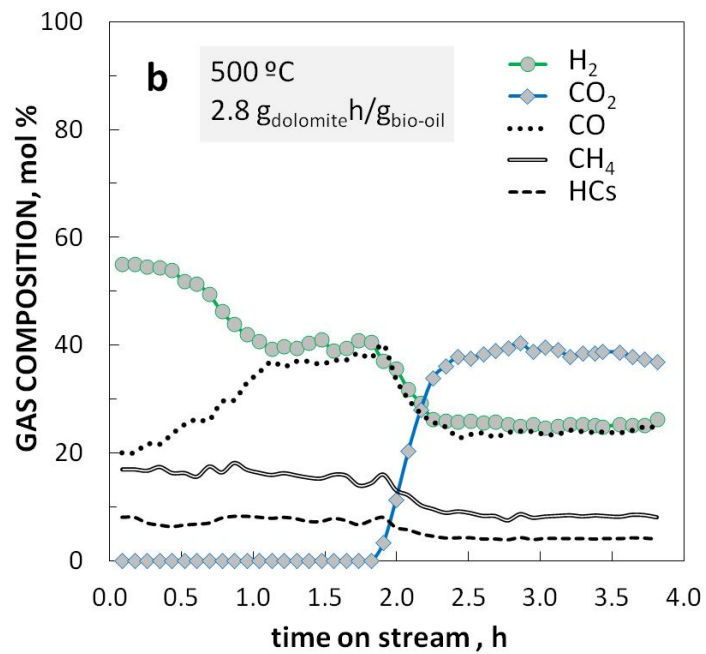
3

4

**Figure 4**



1



2

3

4

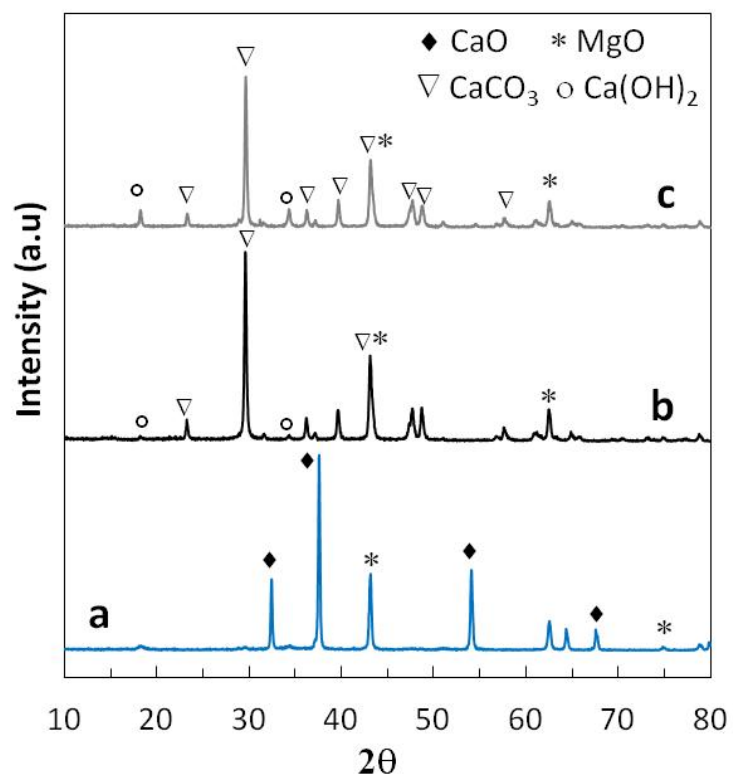
5

6

7

Figure 5



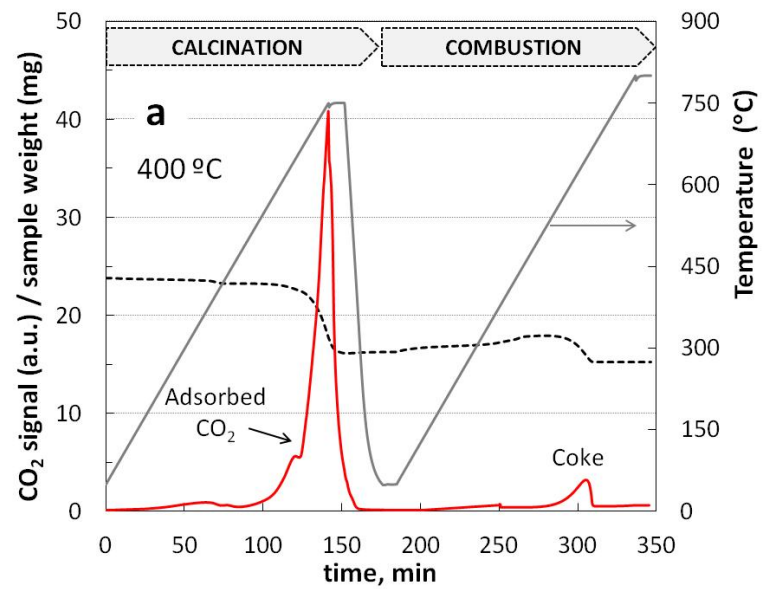
**Figure 6**

1  
2  
3

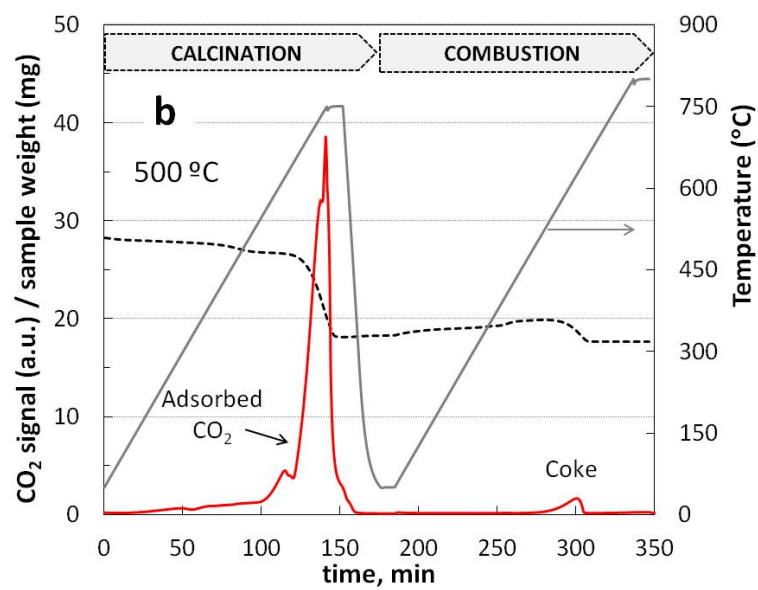
1

2

3



4



5

6

7

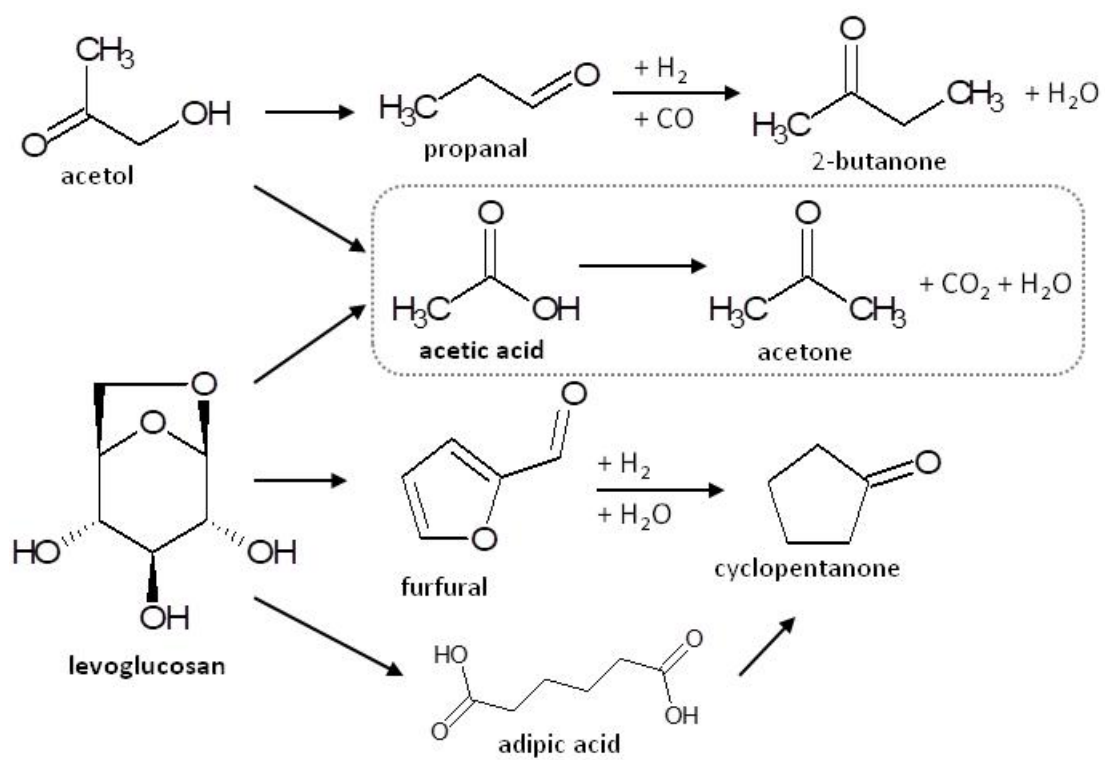
8

9

10

**Figure 7**

1



2

3

4

Figure 8

1

## TABLES

2 **Table 1.** Semi-quantitative composition (% area) of raw bio-oil, liquid collected without  
 3 catalyst (thermal treatment at 400 °C), and upgraded bio-oil produced  
 4 throughout reaction with 2.8 g<sub>dolomite</sub>/h/g<sub>bio-oil</sub> at 400 °C.

	RAW BIO-OIL	Thermal 400 °C	UPGRADED BIO-OIL		
			0.5 h	2 h	4 h
ACIDS	10.0	23.1	-	0.5	3.8
<i>(Acetic)</i>	<i>(8.0)</i>	<i>(21.1)</i>	-	-	-
KETONES	20.4	27.1	81.1	70.5	48.1
LINEAR	15.0	20.4	43.5	36.9	22.1
<i>(Acetol)</i>	<i>(5.6)</i>	<i>(15.2)</i>	-	-	-
<i>(Acetone)</i>	<i>(5.6)</i>	<i>(2.1)</i>	<i>(26.2)</i>	<i>(20.0)</i>	<i>(10.1)</i>
<i>(2-butanone)</i>	<i>(0.3)</i>	<i>(1.8)</i>	<i>(10.9)</i>	<i>(9.3)</i>	<i>(4.2)</i>
CYCLIC	5.4	6.7	37.5	33.6	26.0
<i>(C5 ring)</i>	<i>(4.2)</i>	<i>(5.7)</i>	<i>(30.4)</i>	<i>(27.5)</i>	<i>(20.1)</i>
ESTERS	3.7	4.7	-	0.2	0.6
FURANONES	6.9	3.8	-	4.3	2.3
ALCOHOLS	4.1	4.9	7.1	10.8	5.7
ALDEHYDES	5.0	9.8	6.1	6.2	5.1
<i>(Acetaldehyde)</i>	-	<i>(0.8)</i>	<i>(2.9)</i>	<i>(3.0)</i>	<i>(2.4)</i>
<i>(Furaldehydes)</i>	<i>(3.8)</i>	<i>(5.2)</i>	-	<i>(0.6)</i>	<i>(0.8)</i>
ETHERS	1.9	-	0.8	0.6	1.3
ANHYDROSUGARS	21.4	13.6	-	-	-
<i>(Levoglucozan)</i>	<i>(14.4)</i>	<i>(11.1)</i>	-	-	-
PHENOLS	26.7	12.9	4.9	5.1	29.2
<i>Alkyl-phenols</i>	2.8	0.9	4.9	4.4	14.3
<i>Guaiacols</i>	12.4	6.4	-	0.3	12.2
<i>Catechols</i>	6.4	3.7	-	0.4	1.5
<i>Siringols</i>	0.1	0.2	-	-	-
<i>Naphtalenols</i>	-	-	-	-	1.1
<i>Other</i>	4.8	1.7	-	-	0.1
C <sub>5</sub> -C <sub>12</sub> ALIPHATICS	-	-	-	1.9	3.9

5

6

1 **Table 2.** Semi-quantitative composition (% area) of raw bio-oil, liquid collected without  
 2 catalyst (thermal treatment at 500 °C), and upgraded bio-oil produced  
 3 throughout reaction with 2.8 g<sub>dolomite</sub>h/g<sub>bio-oil</sub> at 500 °C.

	RAW BIO-OIL	Thermal 500 °C	UPGRADED BIO-OIL		
			0.5 h	2 h	4 h
ACIDS	10.0	28.3	-	0.8	5.5
<i>(Acetic)</i>	<i>(8.0)</i>	<i>(22.5)</i>	-	-	-
KETONES	20.4	28.1	83.5	64.7	43.9
LINEAR	15.0	20.6	63.0	45.4	30.3
<i>(Acetol)</i>	<i>(5.6)</i>	<i>(15.4)</i>	-	-	-
<i>(Acetone)</i>	<i>(5.6)</i>	<i>(2.2)</i>	<i>(37.1)</i>	<i>(27.0)</i>	<i>(13.4)</i>
<i>(2-butanone)</i>	<i>(0.3)</i>	<i>(1.6)</i>	<i>(18.6)</i>	<i>(10.8)</i>	<i>(7.6)</i>
CYCLIC	5.4	7.5	20.5	19.3	13.5
<i>(C5 ring)</i>	<i>(4.2)</i>	<i>(7.5)</i>	<i>(17.4)</i>	<i>(18.2)</i>	<i>(13.2)</i>
ESTERS	3.7	3.5	-	0.6	0.4
FURANONES	6.9	3.4	-	0.2	1.5
ALCOHOLS	4.1	3.1	1.1	1.5	0.8
ALDEHYDES	5.0	10.5	0.8	5.7	6.6
<i>(Acetaldehyde)</i>	-	<i>(1.4)</i>	-	<i>(4.1)</i>	<i>(3.0)</i>
<i>(Furaldehydes)</i>	<i>(3.8)</i>	<i>(4.3)</i>	<i>(0.3)</i>	<i>(0.7)</i>	<i>(2.1)</i>
ETHERS	1.9	-	-	0.6	2.4
ANHYDROSUGARS	21.4	10.0	-	-	1.0
<i>(Levogluconan)</i>	<i>(14.4)</i>	<i>(8.1)</i>	-	-	-
PHENOLS	26.7	13.2	7.3	21.4	35.1
<i>Alkyl-phenols</i>	2.8	1.3	7.3	14.9	17.1
<i>Guaiacols</i>	12.4	3.4	-	3.7	3.6
<i>Catechols</i>	6.4	7.5	-	1.9	12.1
<i>Siringols</i>	0.1	-	-	-	-
<i>Naphtalenols</i>	-	-	-	0.9	2.1
<i>Other</i>	4.8	1.0	-	-	0.2
C <sub>5</sub> -C <sub>12</sub> ALIPHATICS	-	-	7.3	4.4	3.0

4

5

6 **Table 3.** Characteristics of deactivated dolomite: surface area (m<sup>2</sup>/g), amount of carbon  
 7 adsorbed (gC/g<sub>dolomite</sub>) and coke deposited (gC/g<sub>dolomite</sub>).

	400 °C	500 °C
Surface area (m <sup>2</sup> /g)	16.8	9.7
C adsorbed (gC/g <sub>dolomite</sub> )	0.15	0.16
Coke deposited (gC/g <sub>dolomite</sub> )	0.12	0.08

8

9